

Molecular and Isotope Analyses of Organic Matter in a Primitive Clast in the Zag H Chondrite

Molecular and Isotope Analyses of Organic Matter in a Primitive Clast in the Zag H Chondrite

*癸生川 陽子¹、伊藤 元雄²、Zolensky Michael³、中藤 亜衣子⁴、菅 大暉⁵、高橋 嘉夫⁶、武市 泰男^{7,8}、間瀬 一彦^{7,8}、Chan Queenie⁹、Fries Marc³、小林 憲正¹

*Yoko Kebukawa¹, Motoo Ito², Michael E. Zolensky³, Aiko Nakato⁴, Hiroki Suga⁵, Yoshio Takahashi⁶, Takeichi Takeichi^{7,8}, Kazuhiko Mase^{7,8}, Queenie H. S. Chan⁹, Marc Fries³, Kensei Kobayashi¹

1. 横浜国立大学 大学院工学研究院、2. 海洋研究開発機構 高知コア研究所、3. ARES, NASA Johnson Space Center、4. 京都大学大学院 理学研究科 地球惑星科学専攻、5. 広島大学大学院理学研究科、6. 東京大学大学院理学系研究科地球惑星科学専攻、7. 高エネルギー加速器研究機構 物質構造科学研究所、8. 総合研究大学院大学 物質構造科学専攻、9. Planetary and Space Sciences, Department of Physical Sciences, The Open University

1. Faculty of Engineering, Yokohama National University, 2. Kochi Institute for Core Sample Research JAMSTEC, 3. ARES, NASA Johnson Space Center, 4. Kyoto University, Division of Earth and Planetary Sciences, 5. Graduate School of Science, Hiroshima University, 6. Department of Earth and Planetary Science, Graduate School of Science, The University of Tokyo, 7. Institute of Materials Structure Science, High-Energy Accelerator Research Organization (KEK), 8. Department of Materials Structure Science, SOKENDAI (The Graduate University for Advanced Studies), 9. Planetary and Space Sciences, Department of Physical Sciences, The Open University

The Zag meteorite is a halite-bearing H3-6 chondrite [1]. The Zag contains xenolithic clast with abundant organic matter which was proposed to be originated from Ceres [2,3]. Here we report coordinated organic analyses by STXM-XANES and NanoSIMS, in order to understand the nature and origin of the organic matter. Our systematic research of the Zag clast may also provide an important linkage to the recent remote sensing observations obtained by the DAWN mission to Ceres [e.g., 4,5].

Carbon-rich areas were located in the clast grains separated from the Zag meteorite with SEM-EDS, and then lift-out sections were prepared with a FIB instrument. C, N, O-X-ray absorption near-edge structure (C,N,O-XANES) spectra of the sections (~100 nm-thick) were obtained using scanning transmission X-ray microscopes (STXM) on beamline 5.3.2.2 at Advanced Light Source, Lawrence Berkeley National Laboratory, and BL-13A at the Photon Factory, KEK. Subsequently, H, C, N, O isotopic images were collected using a CAMECA NanoSIMS 50L ion microprobe.

The STXM elemental map of C-rich region of the Zag clast shows that sub-micrometer organic grains were scattered over the FIB section, some of which have a vein-like structure. The organic matter was somewhat associated with Fe (probably Fe-sulfides). The Fe (+Ni) and C association was also observed in the clasts in Sharps (H3.4) chondrite, suggesting a potential of catalytic gas-solid reactions such as Fischer-Tropsch type (FTT) synthesis [6,7].

C-XANES spectra of the organic grains showed large peaks at 285.2 eV assigned to aromatic carbon, and at 290.3 eV assigned to carbonate (either organic or inorganic), with some features at 287.4 eV (enol C=C-OH), and 287.9 eV (aliphatic), and 288.8 eV (carboxyl). The C-XANES spectra have some similarity with organic matter from Comet Wild 2, rather than with primitive chondritic IOM [8], except for the abundant carbonate in the Zag clast.

NanoSIMS isotope imaging analyses revealed that $\delta^{15}\text{N}$ and δD have highly heterogeneous distributions within the organic matter. The average $\delta^{15}\text{N}$ value was 393 ± 82 ‰ with a hot spot (2639 ± 722 ‰), and the average δD value was 813 ± 206 ‰ with a hot spot ($4,150 \pm 1,710$ ‰). The $\delta^{15}\text{N}$ was similar to the

value of insoluble organic matter (IOM) from Bells (an unusual CM chondrite) and CRs, although δD was less than these IOM [9]. It may indicate that some hydrogen have been exchanged with isotopically light water in the clast parent body.

Both molecular structure and isotopic signatures indicated highly pristine (less altered) nature of organic matter in the clast, and it may be related to cometary organics and/or primitive chondritic IOM.

References: [1] Zolensky M. E. et al. (1999) *Science*, 285, 1377–1379. [2] Fries M. et al. (2013) *76th MetSoc*, Abstract #5266. [3] Zolensky M. E. et al. (2015) *78th MetSoc*, Abstract #5270. [4] Nathues A. et al. (2015) *Nature*, 528, 237–240. [5] De Sanctis M. C. et al. (2015) *Nature*, 528, 241–244. [6] Brearley A. J. (1990) *Geochim. Cosmochim. Acta*, 54, 831–850. [7] Kebukawa Y. et al. (2017) *Geochim. Cosmochim. Acta*, 196, 74–101. [8] Cody G. D. et al. (2008) *Meteorit. & Planet. Sci.*, 43, 353–365. [9] Alexander C. M. O' D. et al. (2007) *Geochim. Cosmochim. Acta*, 71, 4380–4403.

キーワード：隕石、有機物、同位体

Keywords: Meteorite, Organic matter, Isotope

CMコンドライト中の始原水の酸素同位体比

Oxygen isotopic ratio of the primordial water in CM chondrites

*藤谷 渉¹

*Wataru Fujiya¹

1. 茨城大学 理学部

1. Ibaraki University, College of Science

CM chondrites are aqueously altered to various degrees in their parent body. Water ice accreted on the CM parent body reacted with primary anhydrous rock and organic matter producing secondary minerals. The O and H isotopic ratios of the primordial water are key constraints on its origin, however, they are still not well-constrained due to complex isotope exchange between water, rock, and organic matter during the aqueous alteration. Here I investigate the O isotopic ratio of the primordial water in CM chondrites based on bulk O isotopic ratios of CM chondrites and H abundances of their phyllosilicate. Most of the O and H data are from Clayton and Mayeda (1999) and Alexadner et al. (2013).

CM Falls show an apparent correlation between bulk $\delta^{18}\text{O}$ values and H abundances of their phyllosilicate. The regression line of the CM Falls passes through the representative compositions of anhydrous silicate and phyllosilicate matrix in CM chondrites, indicating a mixing line between these two components as endmembers. This well-defined mixing line strongly indicates that the O isotopic ratios of bulk CM chondrites reflect variable amounts of anhydrous silicate and phyllosilicate, i.e., degrees of alteration. A consequence from the mixing line is that phyllosilicate in CM chondrites must have a common O isotopic ratio irrespective of their alteration degrees.

Oxygen isotopic ratios of phyllosilicate are dependent not only on alteration degrees but also on water/rock ratios. Here alteration degrees (f) are evaluated as fraction of anhydrous silicate reacted, and water/rock ratios (x) are expressed as ratios of O moles in water to those in anhydrous rock. In a closed system alteration model by Clayton and Mayeda (1999), O isotopic ratios of phyllosilicate are expressed as a function of f/x based on a mass balance calculation of water, anhydrous silicate, and phyllosilicate. If there is enough water to completely alter anhydrous rock (i.e., large x), then f can range from 0 to 1. In contrast, if anhydrous rock remains after complete consumption of water (i.e., small x), f cannot reach to 1 but only take values smaller than 1 depending on x . Thus, f/x values have a maximum, when water is completely consumed by the aqueous alteration and O isotopic ratios of phyllosilicate should be the same. Given apparent occurrence of anhydrous silicate that remains unaltered, water/rock ratios are likely a limiting factor for the alteration degrees of CM chondrites. Complete water consumption is thus the most straightforward explanation for the similar O isotopic ratios inferred for CM phyllosilicate. Neither alteration temperatures nor hydration reaction considered in the calculation does this conclusion rely on. If no water remained in the system after the aqueous alteration, water/rock ratios of individual CM chondrites can be deduced from H abundances of their phyllosilicate. The deduced x values range from 0.11 to 0.29 (0.19–0.49 by volume ratios). The variable water/rock ratios would suggest heterogeneous water ice accretion on the CM chondrite parent body.

An important implication from this scenario is the O isotopic ratio of the primordial water. In an O three-isotope plot, the O isotopic ratio of CM phyllosilicate should be on the line connecting the O isotopic ratios of the anhydrous silicate and the primordial water. Based on the mass-balance calculation by Clayton and Mayeda (1999), the inferred $\delta^{18}\text{O}$ and $\delta^{17}\text{O}$ values of the primordial water are ~ 65 and ~ 43 ‰, respectively. These estimates depend on hydration reaction considered in the calculation.

キーワード : 水質変質、CMコンドライト、酸素同位体比、始原水

Keywords: Aqueous alteration, CM chondrite, Oxygen isotopic ratio, Primordial water

Carbonate stardust from the Murchison meteorite

*工藤 賢太郎¹

*Kentaro Kudo¹

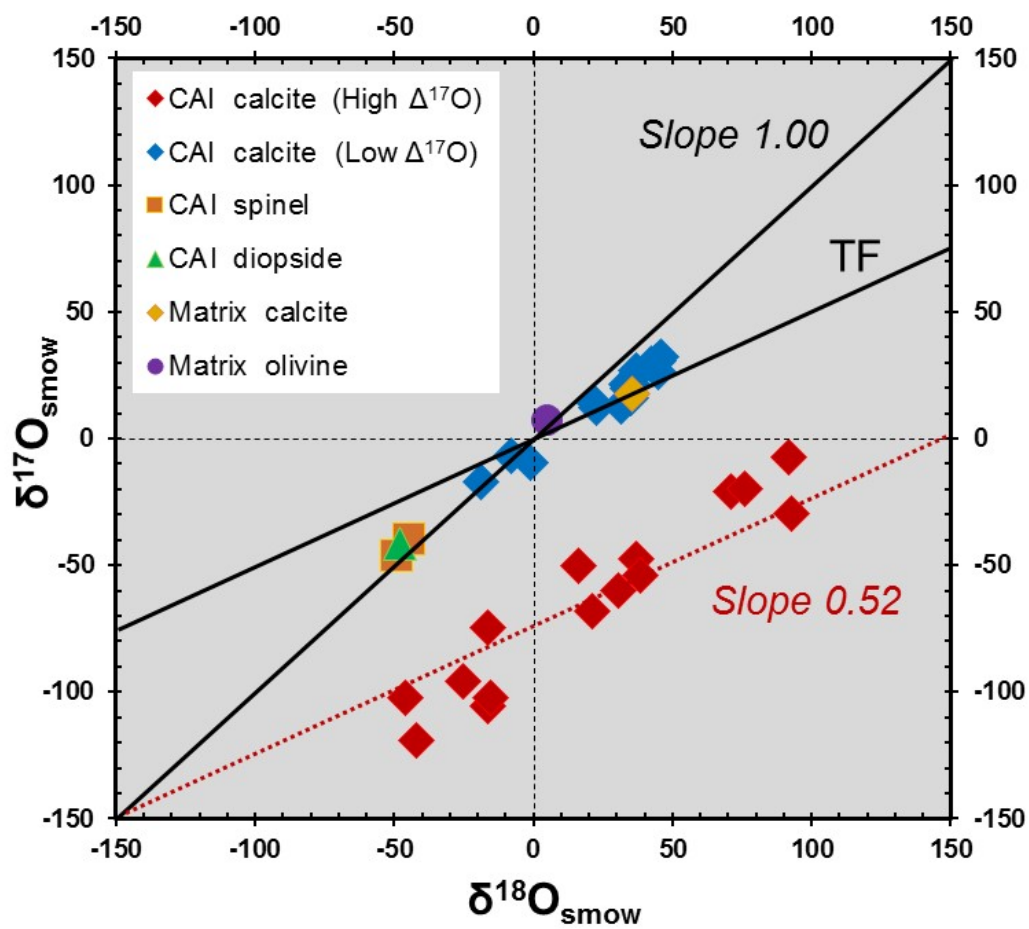
1. 株式会社テクノプロ テクノプロR & D社

1. TechnoPro, Inc. TechnoPro R&D Company

The formation of carbonates in meteorites is generally attributed to secondary aqueous alteration in “planetary environments” (such as Earth, Mars and asteroids), and carbonates are considered to be a good indicator of the past presence of liquid water. However, we report the first discovery of unique calcite grains embedded in the interior of a large calcium-aluminum-rich inclusion (CAI) from the Murchison CM2 carbonaceous chondrite. The individual calcite grains in the CAI are agglomerated submicron ($<1 \mu\text{m}$) crystals and coexist with high-temperature condensates such as spinel and diopside. The oxygen isotope ratios of the calcite grains have an extreme $^{17}\text{O}/^{16}\text{O}$ and $^{18}\text{O}/^{16}\text{O}$ anomaly and are clearly different from that of the secondary carbonates in the matrix. The calcite crystals have large negative anomalies with relatively heterogeneous oxygen isotope compositions ranging from -120 to $+5\text{‰}$ for $\delta^{17}\text{O}_{\text{SMOW}}$ and from -50 to $+100\text{‰}$ for $\delta^{18}\text{O}_{\text{SMOW}}$, which are extremely depleted in ^{17}O and enriched in ^{18}O relative to spinel and diopside (-45 to -40‰ for $\delta^{17}\text{O}_{\text{SMOW}}$ and -50 to -45‰ for $\delta^{18}\text{O}_{\text{SMOW}}$). Although the oxygen isotope compositions of the secondary carbonates are distributed along the TF line, those of the calcite grains in the CAI are heterogeneous and linearly distribute neither on the TF line nor near the TF line in the three oxygen isotope diagram. Therefore, our results suggest that the primitive carbonate grains may form in the proto-solar “nebular environment” without liquid water.

キーワード：酸素同位体、CAI、分子雲、原始太陽、原始太陽系星雲、二次イオン質量分析計

Keywords: Oxygen isotopes, Calcium-aluminium-rich inclusion, Molecular cloud, Proto-sun, Early solar nebula, Nano-SIMS



Variable shock deformation within the CV3 chondrites based on chondrule shapes determined by X-ray tomography and modes of chondrite components

*青木 鍊¹、Fagan Timothy¹、上梶 真之²、土山 明³

*Ren Aoki¹, Timothy J. Fagan¹, Masayuki Uesugi², Akira Tsuchiyama³

1. 早稲田大学理工学術研究院創造理工学部地球環境資源工学科惑星科学研究室、2. 公益財団法人高輝度光科学研究センター、3. 京都大学大学院理学研究科地球惑星科学専攻

1. Department of Resources and Environmental Engineering School of Creative Science and Engineering Waseda University, 2. Japan Synchrotron Radiation Research Institute, 3. Division of Earth and Planetary Sciences, Graduate School of Science, Kyoto University

Introduction: The high abundance of Fe,Ni-metal and high Fo-contents of olivine led to the recognition that the CV3 chondrites Efremovka, Leoville and Vigarano formed at relatively low oxygen fugacities as reduced CV3s (CV3red; [1,2]). In contrast, the CVs Allende and Axtell have little to no Fe,Ni-metal and are classified as an oxidized subgroup (CV3oxA). The CV3red subgroup is characterized by lower metamorphic grades and lower porosities than CV3oxA [3,4]. It has been proposed that the lower metamorphic grade of CV3red is due to an early impact event on the CV3 parent body that lowered porosities [5] and expelled ice [6]. In this study, we test the interpretation that the CV3red subgroup was preferentially deformed by shock by comparing (1) modes of chondrite components, (2) chondrule shapes and (3) clustering of chondrule orientations in a set of CV3red and CV3oxA chondrites.

Methods: We used elemental and BSE maps and photomicrograph mosaics of polished thin sections (pts) to determine modes of chondrite components (chondrules, CAIs, AOAs, matrix) in: one pts of Leoville; two pts of Efremovka; three pts of Vigarano; two pts of Allende and one pts of Axtell. We also determined 2-D shapes and orientations of chondrules in these pts.

Three-dimensional shapes and orientations of chondrules and chondrule-like objects were determined by X-ray computed tomography (CT) in small samples of Efremovka, Vigarano and Allende. X-ray CT data were collected using X-ray CT scanner at Kyoto University (ELESCAN, NX-NCP-C80-I; Nittetsu Elex Co.) [7]. The X-ray CT data consist of a series of 2-D images, in which pixel brightness correlates with linear attenuation coefficient (LAC) [7-8]. Elliptical shapes of low-LAC chondrules and chondrule-like objects were traced on a layer overlying each X-ray CT layer. The subsets of images of traced layers were processed using SLICE software [9] to investigate their shape using tri-axial ellipsoidal approximation and orientation of each axis of chondrules and chondrule-like objects in the samples.

Results: The ratios of matrix/inclusions ("inclusions" = chondrules + CAIs + AOAs) show a trend that correlates with the porosities of [4]. Matrix/inclusions ratios are near 0.3-0.4 for Efremovka and Leoville (porosities approx., 0.6-2%), 0.6-0.7 for Vigarano (porosity, 8%), and 0.9-1.0 for Allende (porosity, 22%). Our Axtell (porosity, 23% [4]) pts has matrix/inclusions ratio = 0.7, but a large CAI probably causes the ratio of the pts to be lower than that of Axtell as a whole. Ebel et al. [10] also found matrix/inclusions lower in Leoville and Vigarano than in Allende; however, their matrix/inclusions ratio for Allende (1.3) is higher than our results.

The 2-D pts data suggest and the 3-D X-ray CT data show that Allende chondrules tend to be spherical, and that the Efremovka and Vigarano chondrules tend to be oblate. Furthermore, the Efremovka and Vigarano chondrules have short axes with well-defined preferred orientations, consistent with flattening. The chondrite component modes, and chondrule shapes and orientations support the interpretation that the CV3red chondrites were affected by an early shock event that limited fluid-rock interaction during subsequent metamorphism [5,6]. Vigarano does not appear to be as strongly shocked as Efremovka and

Leoville.

[1] McSween H.Y. (1977) *GCA* 41, 1777-1790. [2] Weisberg M.K. et al. (2006) *MESS 2*, Lauretta D.S. and McSween H.Y. (eds.) p. 19-52. [3] Bonal L. et al. (2006) *GCA* 70, 1849-1863. [4] Macke R.J. et al. (2011) *MaPS* 46, 1842-1862. [5] Rubin A.E. (2012) *GCA* 90, 181-194. [6] MacPherson G.J. and Krot A.N. (2014) *MaPS* 49, 1250-1270. [7] Tsuchiyama A. et al. (2002) *Geoch.J.* 36, 369-390. [8] Uesugi M. et al. (2013) *GCA* 116, 17-32. [9] Nakano T. et al. (2006) Japan Synchrotron Radiation Research Institute. <http://www-bl20.spring8.or.jp/slice/>. [10] Ebel D.S. et al. (2016) *GCA* 172, 332-356.

キーワード : CVコンドライト、衝突変形、X線断層撮影法

Keywords: CV chondrites, shock deformation, X-ray tomography

Chondrule-cored aggregates (ChCAs): A new rock-type in CV chondrites with implications for timing of high-T crystallization events in the solar nebula

*安田 俊樹¹、Fagan Timothy¹、Krot Alexander²、Kazu Nagashima²

*Toshiki Yasuda¹, Timothy Fagan¹, Alexander N. Krot², Kazu Nagashima²

1. 早稲田大学、2. ハワイ大学

1. Waseda University, 2. University of Hawai'i

Introduction: Ca-Al-rich inclusions (CAIs) and amoeboid olivine aggregates (AOAs) formed by high-temperature reactions between gas and solids, and in some cases liquids, in a hot (ambient temperature > 1400K) region of the protoplanetary disk during initial stages of its evolution [1]. CAIs and AOAs in chondrites of petrologic types ≤ 3.0 tend to be ^{16}O -rich ($\Delta^{17}\text{O}$ -20‰). In contrast, chondrules formed at lower ambient temperatures (<900K) and tend to be ^{16}O -poor compared to CAIs ($\Delta^{17}\text{O}$ -10‰). Most chondrules appear to have postdated formation of CAIs and AOAs, though initial stages of chondrule formation might have overlapped with CAIs and AOAs [2,3]. Because of the later formation age of many chondrules, relict CAIs may be found included within chondrules [4], but chondrule fragments included in CAIs are very rare [5].

In this project, we describe minerals, textures and oxygen isotopes of three unusual objects from the CV3 chondrites Allende and Vigarano in which relict chondrule phenocrysts are partially enclosed by granular olivine texturally similar to AOAs. We refer to these objects as chondrule-cored aggregates (ChCAs). They are significant because their textures suggest the opposite of the conventionally accepted timing; namely, in ChCAs, an early stage of chondrule formation was apparently followed by a later stage of olivine condensation.

Methods: Two ChCAs (called NE-27 and SW-7) were identified in Allende, and one (NW-30) was found in Vigarano. Minerals and textures were characterized using petrographic microscopes, a scanning electron microscope (Hitachi S-3400N) and a JEOL JXA 8900 electron probe micro-analyzer (EPMA) at Waseda University. Oxygen isotopic compositions of olivine in the Allende ChCAs were collected using the Cameca ims-1280 SIMS at University of Hawai'i using conditions similar to those described in [6]. Typical uncertainty including internal and external errors is $\sim 0.6\%$ in both $d^{17}\text{O}$ and $d^{18}\text{O}$.

Results: In Allende ChCA NE-27, a large (>200 μm across), low-Ca pyroxene ($\text{En}_{98}\text{Wo}_1$) similar to a chondrule phenocryst occurs in the core. The relict phenocryst is rimmed by granular olivine grains approximately < 20 μm across. The olivine grains are zoned with cores as Mg-rich as Fo_{95} and rims of approximately Fo_{60} . Olivines with compositions near Fo_{60} also occur in veins that cut across relict pyroxene. ChCA SW-7 has similar low-Ca pyroxene, granular olivine and vein olivine, but is composed of several nodules and has a more diffuse boundary with the Allende matrix. Vigarano ChCA NW-30 also has a core of low-Ca pyroxene. The granular olivine layer is not as complete as in the Allende ChCAs, but granular olivine does appear to replace low-Ca pyroxene near margins of ChCA NW-30.

SIMS oxygen isotope analyses of granular olivine from the Allende ChCAs fall near the Carbonaceous Chondrite Anhydrous Mineral and Primary Chondrule Mineral reference lines (see [7]) and form a spread of $\Delta^{17}\text{O}$ values from -8 to -3‰. All measurements are from MgO-rich cores and avoid FeO-rich olivine rims. The ^{16}O -poor isotopic composition indicates that the olivine rims of ChCAs did not form in a typical AOA-like setting. Regardless of O-isotopic setting, the ChCAs indicate (1) an early episode of chondrule formation, followed subsequently by (2) fragmentation or some process that released pyroxene phenocrysts from their host chondrules, (3) crystallization of granular olivine grains on the margins of

relict phenocrysts, and (4) formation of Fe-rich olivine on rims of grains and in veins during metamorphism.

References: [1] Krot et al. (2009) *GCA* 73, 4963-4997. [2] Kita N.T. et al. (2005) in Krot et al. (eds) *Chondrites and the Protoplanetary Disk*, p. 558- 587. [3] Connelly et al. (2012) *Science* 338, 651-655. [4] Krot A.N. et al. (2007) *MaPS* 42, 1197-1219. [5] Itoh and Yurimoto. (2003) *Nature* 423, 728-731. [6] Nagashima K. et al. (2014) *GCA* 151, 49-67. [7] Ushikubo T. et al. (2012) *GCA* 90, 242-264.

キーワード：コンドリュール、太陽系星雲、酸素同位体

Keywords: chondrules, solar nebula, oxygen isotopes

Development of Laser Post-Ionization SNMS for In-Situ U-Pb chronology

*松田 貴博¹、河井 洋輔¹、宮 晃平¹、青木 順¹、本堂 敏信¹、石原 盛男¹、豊田 岐聡¹、中村 亮介²、寺田 健太郎¹

*Takahiro Matsuda¹, Yosuke Kawai¹, Kohei Miya¹, Jun Aoki¹, Toshinobu Hondo¹, Morio Ishihara¹, Michisato Toyoda¹, Ryosuke Nakamura², Kentaro Terada¹

1. 大阪大学大学院理学研究科、2. 大阪大学産学連携本部

1. Graduate School of Science, Osaka University, 2. Office for University-Industry Collaboration, Osaka University

In space and planetary sciences, Secondary Ion Mass Spectrometer (SIMS) has been widely used for isotopic analyses at the micron scale. In the SIMS analysis, the surface of a sample is irradiated by a primary ion beam, and secondary ions of the sputtered materials are introduced into the mass spectrometer. However, the secondary ion yield of SIMS is very low (less than a few %). As a result, a large amount of material is wasted as neutral particles. In order to improve this disadvantage, we have been developing a Sputtered Neutral Mass Spectrometer (SNMS) with a femto-second laser.

The instrument consists of a focused ion beam system with a liquid metal gallium ion source (Ga-FIB) to attain an ultrahigh lateral resolution less than 1 μm . After a sputtering by Ga-FIB, the sputtered secondary particles are ionized by irradiating the femto-second laser. The post-ionized ions are introduced into the multi-turn ToF analyzer (MULTUM) which achieves ultrahigh mass resolving power of 20000. In addition, we introduced a new detection method, ion counting system, to improve the detection sensitivity. As a result of measurement of a standard sample in U-Pb chronology, 91500 zircon (concentration of uranium is about 100 ppm), the signal peaks of uranium and uranium oxides could be detected, so we have confirmed that the detection limit of the present system is 100 ppm.

In this study, we measured cyrtolite which contains a high concentration of uranium (2 wt.%) and 91500 zircon to confirm whether SNMS can be applied to in-situ U-Pb chronology. As a result of measuring two samples, uranium, uranium oxides and lead signal peaks were detected. In addition, signal peaks of interfering ions, for example, hafnium oxides and gallium clusters, were separated from the peaks of lead by increasing the number of cycles in MULTUM. After the measurement, the diameter of the sputtered area was about 1 μm . In this presentation, we will report the present performance of SNMS in in-situ U-Pb chronology.

キーワード : U-Pb年代分析、SIMS、SNMS

Keywords: U-Pb chronology, SIMS, SNMS

惑星物質の高精度 Cr-Ti 安定同位体測定法の開発

Development of high precision Cr-Ti stable isotope measurements for extra-terrestrial materials.

*日比谷 由紀¹、飯塚 毅¹、山下 勝行²、米田 成一³、山川 茜⁴

*Yuki Hibiya¹, Tsuyoshi Iizuka¹, Katsuyuki Yamashita², Shigekazu Yoneda³, Akane Yamakawa⁴

1. 東京大学大学院理学系研究科、2. 岡山大学大学院自然科学研究科、3. 国立科学博物館理工学研究部、4. 国立環境研究所環境計測研究センター

1. Graduate School of Science, The University of Tokyo, 2. Graduate School of Natural and Technology, Okayama University, 3. Department of Science and Engineering, National Museum of Nature and Science, 4. Center for Environmental Measurement and Analysis, National Institute for Environmental Studies

Introduction: Extra-terrestrial materials have highly variable $^{54}\text{Cr}/^{52}\text{Cr}$ and $^{50}\text{Ti}/^{47}\text{Ti}$ that do not follow mass-dependent fractionation. These variations are considered to reflect nucleosynthetic heterogeneities, possibly resulting from the incomplete and/or impermanent mixing of nuclides from different nucleosynthetic sources (e.g., 1-2). In recent years, these variations have become powerful tools for tracing astrophysical environments of early solar system (e.g., 3-4). They also provide important information about the genetic relationship between the planetary materials especially when the two isotope systems are combined (5). Here, we report the first sequential chemical separation procedure for high-precision Cr and Ti isotopic ratio measurements of extra-terrestrial rocks. We also measured Cr stable isotope compositions of the silicate samples processed through the new chemical separation scheme by thermal ionization mass spectrometry (TIMS).

Results & Discussion: Both Cr and Ti were successfully purified for standard rock samples basalt (JB-1b; 15-50 mg) and Juvinas (~20 mg) monomict non-cumulate eucrite using a new four-stage column chromatographic procedure. All the dissolved silicate samples were dried down, and re-dissolved in 2 mL of 6 M HCL for the first step of column chemistry. In the first step, Fe was separated from most elements including Cr and Ti using AG1-X8 anion exchange resin. The recovery rates in this step were 97-100% for Cr, ~100% for Ti, and 0% for Fe, respectively. In the second step, Ti-fraction was separated from Cr-fraction, and matrix elements like Ca were removed using AG50W-X8 cation exchange resin modifying the Ni separation procedure developed by (6). The recovery rates were 89-100% for Cr, 89-92% for Ti and 0% for Ca, respectively. In this step, Ti was about 43-66% left in the Cr-fraction, and Cr was about 1% left in the Ti-fraction. In the third step, Cr-fraction from the second step was further separated from Ti-fraction and purified for most matrix elements (V, Na, Mn, Mg, Na, Sr etc.) using AG50W-X8 cation exchange resin. The recovery rates in this step were 89-100% for Cr, 97% for Ti and 0% for most matrix elements. In this step, Ti and V were removed from the Cr-fraction, and about 1% of Cr and V left in the Ti-fraction. In the last step, Ti-fractions from the second step and the third step were combined, and the Ti-fraction was further purified for V and Cr. This chemical separation follows the procedure using TODGA resin described by (7). The recovery rates in this step were 97% for Ti, and 0% for Cr and V. These steps decrease the problematic isobaric interferences to be sufficiently low: $^{56}\text{Fe}/^{52}\text{Cr}$, $^{51}\text{V}/^{52}\text{Cr}$ and $^{49}\text{Ti}/^{52}\text{Cr}$ in Cr fraction were as low as 7.09×10^{-6} , 7.75×10^{-8} and 4.05×10^{-7} , respectively. The Cr stable isotope analyses yielded $\epsilon^{54}\text{Cr} = 0.16 \pm 0.22$ (2SE) for JB-1b and $\epsilon^{54}\text{Cr} = -0.48 \pm 0.25$ (2SE) for Juvinas. The reliability of the method was verified by the result that $\epsilon^{54}\text{Cr}$ value for geostandard JB-1b is identical to that of Cr standard within the uncertainties. Furthermore, the $\epsilon^{54}\text{Cr}$ value of Juvinas eucrite is identical within analytical uncertainty to the previous reported value ($\epsilon^{54}\text{Cr} = -0.71 \pm 0.12$ (2SE); (8)). The sequential chemical separation scheme developed here allows us to extract Cr and Ti from basaltic

samples with fewer steps than those in the previous study (e.g., 7,9) and with high recovery rates (>80% for all steps). We will apply the method to various extra-terrestrial materials for better understanding of the origin and evolution of the solar system.

References: (1) Trinquier et al. (2009), (2) Qin et al. (2011), (5) Warren, (2011), (6) Yamakawa et al. (2009), (7) Zhang et al. (2011), (8) Trinquier et al. (2007), (9) Schiller et al. (2014)

キーワード：クロム、チタン、核合成異常、化学分離、TIMS、ユークライト隕石
Keywords: Cr, Ti, nucleosynthetic anomaly, chemical separation, TIMS, eucrite

放射光CTを用いた、隕石の総合観察システムの構築

Development of integrated SR-CT method for the total analysis of meteorites

*上梶 真之¹、竹内 晃久¹、上杉 健太郎¹

*Masayuki Uesugi¹, Akihisa Takeuchi¹, Kentaro Uesugi¹

1. 公益財団法人高輝度光科学研究センター

1. Japan synchrotron radiation research institute

Synchrotron radiation computed tomography (SR-CT) enables us to observe the internal structure of extraterrestrial materials with spatial resolution around 100nm three-dimensionally, without breaking them. In previous studies, however, we can not investigate the mineral phases and chemical composition of internal materials of the samples. In addition, considerable errors are occurred if we observed samples larger than the field of view of the CT instruments.

Recently, several methods of the combination of x-ray diffraction (XRD) and CT were developed in the material sciences of engineering fields [e.g. 1-2], and performed precise observation of polycrystalline metals or alloys. We can determine the mineral phases of the sample uniquely, orientation of the crystals inside them and analyze their chemical composition by linear attenuation coefficient [3].

In this paper, we report a new instrument for the total analysis of rocky material which includes XRD, SR-CT, and local tomography which images a region of interest of a sample by zooming up it. We also developed softwares for the integrated analysis of data obtained by the system. The software relates the images and data obtained by those different methods with simple operation. Using this system, we can search and investigate certain materials or minerals included in the sample, such as carbon phases. We also introduce future developments and application for analysis of materials obtained by future sample return missions.

References: [1] Toda et al., (2016) *Acta Materialia* 107 310-324. [2] West et al., (2009) *Scripta Materialia* 61 875-878. [3] Uesugi et al., (2013) *Geochimica et Cosmochimica Acta* 116, 17-32.

キーワード：放射光CT、XRD-CT、隕石

Keywords: synchrotron radiation tomography, XRD-CT, meteorite

吸収・位相トモグラフィーによるMIL090657隕石マトリクスの3次元観察

3D-observation of matrix of MIL 090657 meteorite by absorption-phase tomography

*杉本 美弥菜¹、土山 明¹、松野 淳也¹、三宅 亮¹、中野 司²、上杉 健太郎³、竹内 亮久³、瀧川 晶¹、高山 亜紀子¹、中村メッセンジャー 圭子⁴、バートン アーロン⁴、メッセンジャー スコット⁴

*Sugimoto Miyama¹, Akira Tsuchiyama¹, Junya Matsuno¹, Akira Miyake¹, Tsukasa Nakano², Kentaro Uesugi³, Akihisa Takeuchi³, Aki Takigawa¹, Akiko Takayama¹, Keiko Nakamura-Messenger⁴, Aaron S. Burton⁴, Scott Messenger⁴

1. 京都大学大学院 理学研究科 地球惑星科学専攻、2. 産業技術総合研究所地質情報研究部門、3. 高輝度光科学研究センターSPring-8、4. NASAジョンソン宇宙センター

1. Division of Earth and Planetary Sciences, Graduate School of Science, Kyoto University, 2. AIST/GSJ, 3. JASRI/SPring-8, 4. NASA/JSC

MIL 090657隕石(CR2.7)は水質変成をほとんど受けていない始原的な炭素質コンドライトの一つであり[1], Paris隕石[2]と並んで、マトリクス中に彗星塵に特徴的に含まれるGEMS (glass with embedded metal and sulfide) に類似した非晶質珪酸塩が報告されている。これまでに、この隕石のマトリクスには、サブミクロンサイズの粒状珪酸塩からなる岩相(岩相1), GEMSに類似した非晶質珪酸塩からなる岩相(岩相2), 層状珪酸塩をもつ岩相(岩相3)が報告されており、岩相1, 2には豊富な有機物も存在している[3,4]。また、岩相1, 2は組成や組織の違いによってそれぞれ2種類のサブタイプに細分できる[5]。このような様々な岩相の構成物やそれらの隣接関係を明らかにすることは、原始太陽系星雲や小天体の集積・変成過程を考える上で重要である。

これまでの研究ではSEMやTEMによる2次元観察に限られていたが、本研究では様々な岩相の構成物やそれらの隣接関係を3次元的に明らかにするために、2種類のCT法 (DET[6], SIXM[7]) を用いたMIL 090657隕石マトリクスの観察を行った。DET (dual-energy micro tomography) は、2種類のX線エネルギーでの吸収コントラストから鉱物種を識別する方法であり、SIXM (scanning-imaging x-ray microscopy) は、位相コントラスト像と吸収コントラスト像の同時撮影から有機物のような軽元素からなる物質を識別できる。両者を組み合わせることで、有機物や空隙だけでなく、層状珪酸塩や炭酸塩などの水質変成物の識別も可能となる[8]。

本研究では、MIL 090657隕石マトリクスの欠片 (~100 μm) を樹脂埋めしたpotted buttをFE-SEM/EDSにより詳細に観察・分析し、その結果をもとにして、FIB (FEI Helios NanoLab G3 CX) を用いて岩相1, 2及びその境界から3個のCT用試料 (約30-50 μmサイズのハウス型、以降H1, H3, H5と呼ぶ) を作成した。CT撮影は、放射光施設SPring-8のBL47XUにおいて、DETによる7 keV, 8 keVでの撮影 (画素サイズ: ~40及び~80 nm) と、SIXMによる撮影 (8 keV, 画素サイズ: ~100 nm, H3のみ) を行った。

この結果、岩相1, 2の他に、H1, H3から新たに岩相4, 5, 6を発見した。岩相4, 5, 6のマトリクスは主に鉄の含有量の異なる層状珪酸塩で構成されると考えられる。岩相4には硫化鉄やフランボイダルマグネタイトが見られた。岩相5はマグネタイトや炭酸塩を、岩相6はクラックを持つ無水珪酸塩を内部に含んでいた。岩相1, 2, 4, 5には空隙が多く、岩相6にはほとんど空隙は観察されなかった。岩相4は岩相1と接しており、境界の見分けはつきにくい。岩相2, 5, 6は互いに隣接し、特に岩相6は他の岩相との境界がはっきりしていた。岩相1と岩相2の境界領域を含むH5中には、その両方に金属鉄や輝石などの大きな粒子 (5~10 μm) が存在し、岩相1と2の境界は3次元的にもシャープではなかった。

以上のように、3次元観察により多様な岩相が新たに見出され、MIL 090657隕石は複雑な集積・変成過程を経たことが推察される。水質変成に弱い非晶質珪酸塩をもつ岩相2は最も始原的であり、岩相2と層状珪酸塩からなる岩相 (岩相5, 6) が接していることは、岩相5, 6が水質変成後に岩相2とともに集積したものと考えられる。一方、岩相1と2の境界は明瞭でなく、これらは共通の集積物であり、岩相1は弱い水質変成を受け、その後弱い熱変成[3]を受けた可能性が示唆される。

[1] Davidson et al. 2015, 46th LPSC, 1603. [2] Leroux et al. 2015, GCA, 170: 247-265. [3] Cao et al. 2016, 47th LPSC, 2427. [4] Sugimoto et al. 2016, Goldschmidt Workshop on Experimental Cosmochemistry, 15. [5] 杉本ほか. 2016, 日本鉱物科学会年会講演要旨集, 161. [6] Tsuchiyama et al. 2013, GCA, 116: 5-16. [7] Takeuchi et al. 2013, J. Synch. Rad., 20: 793-800. [8] Tsuchiyama et al. 2017, 48th LPSC, 2680.

キーワード：始原的炭素質コンドライト、非晶質珪酸塩、水質変成

Keywords: primitive carbonaceous chondrite, amorphous silicate, aqueous alteration

霧囲気制御ガス浮遊システムによるコンドリュール組織の再現実験 Reproduction of chondrules using ambient-controlled levitation system

*瀬戸 雄介¹、鈴木 康太¹、庄田 直起¹

*Yusuke Seto¹, Kouta Suzuki¹, Naoki Shoda¹

1. 神戸大学大学院理学研究科

1. Graduate School of Science, Kobe University

Chondrules are round (or irregular) shaped particles with sizes ranging of 0.1 –10 mm. They are mainly composed of silicates, iron metals and iron sulfides, and thought to be formed by the rapid cooling of fully or partially molten droplets before they accreted. They show unique and diverse internal micro-textures (e.g., porphyritic olivine, barred olivine, radial pyroxene, etc.) which reflect not only a composition of the starting material, but also nebular conditions, such as gas species and their partial pressures, heating and cooling rate. The conditions of chondrule formation, however, remain poorly constrained. This is mainly because the reproduction of the chondrule formation processes in a laboratory is experimentally difficult, especially in terms of a container-less arrangement and a reducing (low-fO₂) ambient. In the present study, we developed gas-levitation system embedded in ambient-controlled tube furnace in order to reproduce micro-textures of chondrules, and to constrain their formation conditions.

A summary of the newly developed equipment is as follows. A vertical tube furnace with a silicon carbide heater (double coiled spiral type) and an alumina core tube (OD 50mm, ID 42 mm, referred to as “outer-tube” hereafter) was used as a heating device. An alumina inner core tube (OD 32mm, ID 26 mm, referred to as “inner-tube” hereafter) was inserted into the outer tube, and an amorphous-carbon gas-nozzle (blowout hole diameter of 1 mm) was set on at the top of the inner-tube. H₂+CO₂+Ar mixed gas were separately introduced into the both inner and outer core tubes from a gas port at the bottom of the tubes, and gas flow rates were controlled by digital mass flow controllers. The inner tube with the gas-nozzle can move up and down by a motor-controlled pantograph, and thereby the seamless switching from a sample exchange position to maximum temperature position is possible. Levitated samples were observed by a long focal CCD camera thorough mirrors and infrared filters. To avoid lowering of the image contrast due to incandescence above 1500 K, area around the sample were irradiated by a system of high-power LED (20W) and large-aperture lens.

Using the above system, we demonstrated the containerless cooling experiments for molten silicate droplets. As starting materials, (i) natural peridotite (analogue to a Fe-poor chondrule) and (ii) oxide mixture corresponding to a type IIA (F-rich) chondrule were used. They were melted at (i) 1773 K and (ii) 1673 K for durations of ~5 min and cooled with a rate of 10⁴ K/hr under a reducing condition (log fO₂ = IW-1) in the above system. Surfaces and internal textures of the recovered samples were analyzed using SEM-EDX. In the recovered samples of (i), residues of original olivine (Fa~10) were surrounded by overgrown Fe-poor olivine (Fa6) with zigzag surfaces. In the molten area, both platy (10 μm thickness) and porphyritic (3-20 μm) olivines were observed. Both of them showed distinct chemical zoning and are embedded in Al₂O₃-SiO₂-rich glass. The samples of (ii) were thought to be experienced by fully molten states. They shows also both platy (100 μm thickness) and porphyritic (10-30 μm) olivine embedded in an Al₂O₃-SiO₂-rich glass. Although previous studies suggest that porphyritic chondrules were formed from partially molten states while nonporphyritic chondrules from fully molten states, the present results indicates that porphyritic texture is still possible to be formed from fully molten states. The demonstrations of the present study show that reducing-gas levitation experiments is a powerful

technique to simulate the molten-quenched texture of early solar materials.

キーワード：コンドリュール、ガス浮遊法、急冷組織
Keywords: chondrule, gas levitation, quench texture

Occurrence of Fe in sulfides, silicates and metals in enstatite and ordinary chondrites: Wide ranges in oxidation-reduction due to variations in H₂O gas?

*谷村 佑貴¹、Fagan Timothy¹

*Yuki Tanimura¹, Timothy Fagan¹

1. 早稲田大学教育学部理学科地球科学専修

1. Department of Earth Sciences, School of Education, Waseda University

Introduction: Iron is one of the most abundant elements in solid materials of the solar system, and occurs in chondrites in 3 main mineral groups: silicates, metals, and sulfides [1]. Speciation of Fe between these mineral groups is an indicator of the conditions where chondrites formed in the solar nebula.

Fe-speciation of chondrites between silicates and metal indicates wide variations in oxidation state [1].

Were there similar variations in the extent of sulfidation? In this project, we use Fe speciation among silicates, metal, and sulfides in enstatite, ordinary and Rumuruti-like chondrites to address variations in oxidation, reduction and sulfidation in the part of the solar nebula where these chondrite groups formed.

Methods: We used elemental and BSE maps of polished thin sections (pts) to determine modes of minerals (enstatite, olivine, Fe,Ni-metal, troilite, ...) in: Bensour (LL6), Mt. Tazerzait (L5), Tamdakht (H5), LEW 88180 (EH5), NWA 974 (E6), NWA 953 (R3). Elemental maps were collected using a JEOL JXA-8900 electron probe micro-analyzer (EPMA) at Waseda University (WU). Modes were determined manually using grids overlain on the pts maps in a graphics program. The compositions of major minerals were analyzed using the WU EPMA. We calculated moles of Fe in each mineral using the mineral compositions, published molar volumes and the modes.

We also used wet chemical analyses of chondrite whole rocks from two data sets: one collected and compiled by the Smithsonian Museum, US [2], and the other by the National Institute of Polar Research (NIPR), Japan [3]. In these analyses, FeO, Fe-metal and FeS were determined directly.

A reaction space approach [4,5] was used to identify the main reactions possible between minerals and O- and S-rich gas in E, O and R chondrites. The reacting system consists of the following phases and solid solution vectors: NaAlSi₃O₈, CaMgSi₂O₆, MgSiO₃, AlAlMg₁Si₁, SiO₂, O-rich gas, S-rich gas, FeMg₁, Fe-metal, FeS, CaAlNa₁Si₁ and Mg₂SiO₄. These phases can be described by the components: Na, Ca, Mg, Al, Si, O₂, S₂ and Fe. In this system, all transfers of mass between the silicate, sulfide and metal subsystems can be described as progress along two reactions: (R_m) Mg₂SiO₄ + 2 FeMg₁ = 2 Fe + SiO₂ + O₂; and (R_s) Mg₂SiO₄ + 2 FeMg₁ + S₂ = 2 FeS + SiO₂ + O₂. Increasing reduction is indicated by progress on R_m, increasing sulfidation by progress on R_s, and oxidizing conditions are indicated by minor progress on both reactions. Progress on R_m is designated by X_m and ranges from 0 to 1; likewise, X_s shows progress on R_s. Results: Fe-speciation determined from all three data sets indicate wide variations in FeO/Fe-metal (X_m from 0 to 1) and limited variations in FeO/FeS (X_s mostly from 0.1 to 0.3). The results from most oxidized to most reduced are: R-, LL-, L-, H-, E-chondrites, in agreement with [1].

Considering a model for flow of ice and other materials in the solar nebula [6], the extent of oxidation was high at an evaporation front. In this model, evaporation of H₂O-ice caused the local gas to become enriched in H₂O, increasing the oxygen fugacity of the gas. With more oxygen present in the gas, R_m could proceed to the left, transferring Fe from metal to silicates. The R chondrites could have formed just inside of the evaporation front, where the gas was enriched in H₂O-vapor. Ordinary and enstatite chondrites might have formed farther inward from the evaporation front.

References: [1] McSween H.Y. and Huss G.R. (2010) *Cosmochemistry*, Cambridge, 217-218. [2]

Jarosewich E. (2006) *MaPS* 41:1381-1382. [3] Yanai K. and Kojima H. (1995) *Catalog of the Antarctic Meteorites*, NIPR, 230 p. [4] Thompson J.B. et al (1982) *JPetrol* vol. 23: 1-27. [5] Fagan T.J. and Day H.W. (1997) *Geology* 25: 395-398. [6] Cuzzi J.N. and Zahnle K.J. (2004) *AstrophysicalJ* vol. 614: 490-496.

キーワード : コンドライト隕石、太陽系星雲、酸化還元

Keywords: chondrites, solar nebula, oxidation-reduction

Shock pressure estimation by high-pressure polymorphs and cathodoluminescence spectra of maskelynite in Yamato-790729 L6 chondrite and their significance for collisional condition

加藤 由香子¹、関根 利守^{1,2}、*鹿山 雅裕^{1,3,4}、宮原 正明^{1,3}、山口 亮^{5,6}

Yukako Kato¹, Toshimori Sekine^{1,2}, *Masahiro KAYAMA^{1,3,4}, Masaaki Miyahara^{1,3}, Akira Yamaguchi^{5,6}

1. 広島大学理学研究科地球惑星システム学専攻、2. Center for High Pressure Science and Technology Advanced Research、3. 東北大学大学院理学研究科地学専攻、4. 東北大学学際科学フロンティア研究所新領域創成研究部、5. 国立極地研究所、6. 総合研究大学院大学複合科学研究科極域科学専攻

1. Department of Earth and Planetary Systems Science, Graduate School of Science, Hiroshima University, 2. Center for High Pressure Science and Technology Advanced Research, 3. Department of Earth and Planetary Material Sciences, Faculty of Science, Tohoku University, 4. Creative Interdisciplinary Research Division, Frontier Research Institute for Interdisciplinary Sciences, Tohoku University, 5. National Institute of Polar Research, 6. Department of Polar Science, School of Multidisciplinary Science, SOKENDAI

Most asteroidal meteorites have experienced impact events that occurred on their parent-bodies because shock-induced features (e.g., melting textures, high-pressure polymorphs and vitrification) provide clear evidences for impact events. L6 type ordinary chondrite frequently has a vein-like shock-induced melting texture (a shock-melt vein or shock vein). Furthermore, they may contain high-pressure polymorphs and shock-induced glasses (e.g., maskelynite) that were transformed from the constituent minerals (e.g., olivine, pyroxene and plagioclase) due to high-pressure and -temperature conditions induced by impact events. Such high-pressure polymorphs and shock-induced glasses provide constraints on the asteroidal impact history. In this study, Yamato (Y)-790729, which is classified as heavily shocked L6 type ordinary chondrites, was investigated to estimate the shock-pressure, temperature and size of the parent body, based on high-pressure polymorph assemblage and cathodoluminescence (CL) spectroscopy of maskelynite. The shock pressure conditions estimated by these two methods were also compared each other to evaluate the validity of the methods.

Y-790729 is a typical L6 ordinary chondrite with remnants of chondritic textures, and has a shock-melt vein. The host-rock of Y-790729 consists mainly of olivine, low-Ca pyroxene, feldspar, metallic Fe-Ni, and iron-sulfide with minor phosphate and chromite. Undulatory extinction was recognized in some plagioclase and pyroxene grains under the optical microscope. A scanning electron microscope (SEM), laser micro-Raman spectroscopy and transmission electron microscope (TEM) equipped with an X-ray energy dispersive spectrometer (EDS) were carried out for this meteorite to determine the chemical composition, observe the petrological features and identify the high-pressure phases. Another SEM with a CL spectrometer was also conducted to characterize the shock metamorphic effects of the feldspar and maskelynite.

A shock-melt vein with a width of $< \sim 620 \mu\text{m}$ exists in Y-790729. TEM observations and micro-Raman spectroscopy of this meteorites demonstrated that ringwoodite, majorite, akimotoite, lingunite, tuite, and xieite occurred in and around the shock-melt vein. The ringwoodite is polycrystalline assemblages under the TEM observations, where the individual grain reaches from ~ 0.1 to $\sim 1.3 \mu\text{m}$ across. According to the phase equilibrium diagrams of these high-pressure polymorphs, the shock pressure in the shock-melt vein is about 14-23 GPa.

Part of plagioclase grains in the host-rock occurred as maskelynite under the optical microscope and Raman spectroscopy. Sixteen different CL spectra from maskelynite portions of Y-790729 showed characteristic emission bands at ~ 330 and 380 nm . The obtained CL spectral data of maskelynite portions

were deconvoluted into three emission components at 2.95, 3.26, and 3.88 eV. The intensity of emission component at 2.95 eV was selected as a calibrated barometer to estimate shock pressure, and the results indicate shock pressures of about 11-19 GPa. The difference in pressure between the shock-melt vein and host-rock might suggest heterogeneous shock conditions.

Assuming an average shock pressure of 18 GPa, the impact velocity of parent-body of Y-790729 is calculated to be ~ 1.90 km/s. The melting temperature of the shock vein could be about 2173 K at 18 GPa, according to previous data obtained from the KLB-1 peridotite and Allende meteorite. It is likely that the duration of high-pressure and -temperature conditions recorded in the shock-melt veins of Y-790729 is several seconds, implying that the parent-body size is ~ 10 km in diameter at least, based on the incoherent formation mechanism of ringwoodite in Y-790729.

キーワード : L6普通コンドライト、Yamato-790729、高圧多形、カソードルミネッセンス

Keywords: L6 type ordinary chondrite, Yamato-790729, high-pressure polymorphs, cathodoluminescence

Discovery of heavily shocked type 3 ordinary chondrites

Discovery of heavily shocked type 3 ordinary chondrites

*宮原 正明¹、山口 亮²、大谷 栄治³

*Masaaki Miyahara¹, Akira Yamaguchi², Eiji Ohtani³

1. Department of Earth and Planetary Systems Science, Graduate School of Science, Hiroshima University, 2. NIPR, 3. Department of Earth Sciences, Graduate School of Science, Tohoku University

1. Department of Earth and Planetary Systems Science, Graduate School of Science, Hiroshima University, 2. NIPR, 3. Department of Earth Sciences, Graduate School of Science, Tohoku University

Based on the onion cell model, a parent-body of an ordinary chondrite consists of petrographic type 6, 5, 4 and 3 from inward to outward. A high-pressure polymorph occurring in a shocked ordinary chondrite gives shock pressure, temperature, impact velocity and impactor size, which become clues for understanding a destruction process of an ordinary chondrite parent-body. We have to clarify the inventories of a high-pressure polymorph included in all petrologic types to elucidate the destruction process of an ordinary chondrite parent-body. Accordingly, we will describe the petrologic and mineralogical features of the shock-induced textures and high-pressure polymorphs therein in heavily shocked type 3 ordinary chondrites.

We observed about three hundreds Antarctica type 3 ordinary chondrite (H-, L- and LL-type) petrographic thin sections stored in the NIPR under an optical microscope. We found eight type 3 ordinary chondrites with a distinct melting texture; Y-981139 (H3), A-87170 (L3), A-87220 (L3), Y-000886 (L3), Y-86706 (L3), Y-981327 (L3) A-881199 (LL3.4) and A-881981 (LL3). We also selected thirty three type 3 ordinary chondrite petrographic thin sections without a melting texture as a reference. All these samples were scanned with a field-emission scanning electron microscope (FE-SEM) to observe the fine-textures of melt-pockets and the morphologies of chondrules. Mineralogy was determined by a laser micro-Raman spectroscopy.

FE-SEM observations revealed that the melting textures (melt-pocket) in type 3 always occur around a boundary between a chondrule and matrix. Fine-grained quench silicate crystals and the spherules of metallic iron-nickel + iron sulfide with a eutectic texture filled the melt-pockets. Several interstitial glass fragments were entrained in the melt-pockets of A-881199 (LL3). Their bulk-chemical compositions are similar to that of plagioclase. Based on a Raman spectroscopy analysis, most of them are amorphous. On the other hand, back-scattered electron (BSE) image depicted that one of the interstitial glasses had a granular texture. A strong Raman shifts appeared at 372, 693 and 1032 cm⁻¹ from the interstitial glass with a granular texture, which appear to be those of jadeite (Considering its chemical composition, probably, jadeite-diopside solid-solution) or tssintite. This is a first discovery of a high-pressure polymorph from type 3 ordinary chondrite. The ellipticity of chondrules ($1 - (\text{short axis}/\text{long axis})$) in type 3 chondrites with and without a melting texture was measured. The ellipticity of chondrules in chondrites with a melting texture is ~ 0.31 , which appears to be a bit bigger than those of chondrules in chondrites without a melting texture. The orientation of the long axis of chondrules was also measured. The long axis of chondrules in chondrites with a melting texture appears to be oriented along a specific orientation. The ellipticity and orientation degree of chondrules besides a high-pressure polymorph would be available for estimating shock pressure condition recorded in an ordinary chondrite.

キーワード : ordinary chondrite、 shock、 high-pressure polymorph

Keywords: ordinary chondrite, shock, high-pressure polymorph

Formation process of Fe-FeS globules in melt veins in shocked ordinary chondrites

*谷 理帆¹、富岡 尚敬²、ダス カウシク¹

*Riho Tani¹, Naotaka Tomioka², Kaushik Das¹

1. 広島大学地球惑星システム学科、2. 海洋研究開発機構高知コア研究所

1. Hiroshima University Department of Earth and Planetary Systems Science, 2. Kochi Institute for Core Sample Research, Japan Agency for Marine-Earth Science and Technology

Heavily shocked stony meteorites contain optically black veins called shock veins. The veins consist of micron to submicron-scale grains of silicates, oxides, Fe-Ni metals and Fe-sulfide. During shock vein formation, metal-sulfide melt is not chemically mixed with silicate melt due to their mutual immiscibility. As a result, the metal-sulfide is crystallized as tiny globules in the silicate/oxide matrix in shock veins. Such globules are an unequivocal evidence for extensive melting of silicate materials. Previously, mineralogical studies of shock vein have been mainly focused on silicate and oxide minerals, since these minerals often occur as high-pressure phases. Pressure-temperature histories in shocked chondrites have been deduced from high-pressure mineral assemblages based on experimentally determined phase equilibria [1]. However, metals and sulfides in shock veins have not been well investigated. In the present study, we have examined the Fe-FeS globules in shock veins in two ordinary chondrites (NWA4719 and Tenham), which are considered to have experienced different shock pressures, [2–3] to obtain further information of the formation process of shock veins.

The trend of the globule size in the shock vein shows that it becomes larger from the vein wall to the center (up to 25 μm) due to the difference of cooling rate and local fluid dynamics. Following the previous study [4], cooling rates of shock veins were estimated from spacing of Fe-metal dendrites in the globules by a cooling-rate meter established for Fe-dendrites in alloys [5]. The widths of Fe-dendrites in NWA4719 and Tenham are in the range of $\sim 300\text{--}600$ nm, and estimated cooling rates of the shock veins in are extremely high (10^6 deg C/sec).

To evaluate such a seemingly unrealistically high cooling rate, we examined mineral phases of the globules in Tenham by TEM/STEM. Fe-FeS globules are surrounded by high pressure silicate minerals including aluminous majorite crystallized from chondritic melt at pressures above 14 GPa. Meanwhile, X-ray elemental mapping clarified that the globules consist of grains of kamacite, taenite and troilite (<2 μm in size). But, high-pressure phases of Fe-sulfide such as Fe_3S_2 and Fe_3S , which are stable above ~ 14 and ~ 21 GPa [6,7] respectively, were not found. The results suggest that shock pressure in Tenham was significantly dropped from >14 GPa when temperature of the shock vein was in between the liquidus temperature of silicate (~ 2000 deg C) and eutectic temperature of Fe-FeS (~ 1000 deg C). Therefore, only silicate minerals could have been crystallized as high pressure phases. The absence of high-pressure phases of Fe-sulfide is rather consistent with much slower cooling rate than that estimated by Fe-dendrite spacing. The cooling-rate meter established in metallurgical studies provides overestimated values for shock veins formed in a dynamic high-pressure process.

References: [1] e.g. Agee et al. (1995) *J. Geophys. Res.* 100, 17725–17740. [2] Kimura et al. (2007) *Meteorit. Planet. Sci.* 42, 5139.pdf. [3] e.g. Tomioka and Fujino (1999) *Am. Mineral.* 84, 267–271. [4] Scott (1982) *Geochim. Cosmochim. Acta* 46, 813–823. [5] Flemings et al. (1970) *J. Iron Steel Inst.* 208, 371–381. [6] Fei et al. (1997) *Science* 275, 1621–1623 [7] Fei et al. (2000) *Am. Mineral.* 85, 1830–1833.

キーワード：硫化金属グロビュール、衝撃脈、普通コンドライト、透過型電子顕微鏡
Keywords: metal-sulfide globule, shock vein, ordinary chondrite, TEM

Petrologic evidence for early impact events inferred from differentiated achondrites

*山口 亮¹、白井 直樹²

*Akira Yamaguchi¹, Naoki Shirai²

1. 国立極地研究所、2. 首都大学東京

1. National Institute of Polar Research, 2. Tokyo Metropolitan University

Eucrites, grouped in the HED meteorites are the largest group of differentiated achondrites. There are several achondrites petrologically similar to eucrites but were derived from distinct sources. Detailed petrologic and geochemical studies of such asteroidal achondrites provide better understanding of early igneous, thermal and impact histories of differentiated planetesimals. We report petrology and geochemistry of achondrites, EET 92023 and Dho 007. Oxygen isotopic compositions of these meteorites are significantly shifted away from the eucrite fractionation line. EET 92023 is an unbrecciated achondrite whereas Dho 007 is a polymict breccia mainly composed of medium to coarse-grained granular clasts. These achondrites are mainly composed of low-Ca pyroxene and plagioclase, petrologically similar to normal cumulate eucrites. However, these rocks contain significant amounts of kamacite and taenite not common in unbrecciated, crystalline eucrites. EET 92023 and Dho 007 contain significant amounts of platinum group elements (PGEs) (~10% of CI), several orders of magnitude higher than those of monomict eucrites. We suggest that the metallic phases carrying PGEs were incorporated by projectiles during or before igneous crystallization and thermal metamorphism. The projectiles were likely to be iron meteorites rather than chondritic materials, as indicated by the lack of olivine and the presence of free silica. Therefore, the oxygen isotopic signatures are indigenous, rather than due to contamination of the projectile materials with different oxygen isotopic compositions. A significant thermal event involving metamorphism after the impact event indicates that EET 92023 and Dho 007 record early impact events which took place shortly after the crust formation on a differentiated protoplanet when the crust was still hot.

キーワード：隕石、エコンドライト

Keywords: meteorites, achondrites

A petrographic study of the NWA 2924 mesosiderite

*杉浦 直治¹、木村 真²、荒井 朋子¹、松井 孝典¹

*naoji sugiura¹, makoto kimura², tomoko arai¹, takafumi matsui¹

1. 千葉工業大学、2. 茨城大学

1. Chiba Institute of Technology, 2. Ibaraki University

Recent chronological studies [1,2] revealed that reheating of mesosiderites occurred significantly later (~30 Ma) than the solidification of the magma ocean (~4563 Ma) on the parent body. At this age, ²⁶Al cannot be a significant heat source. Also, metal cannot be the heat source because even if it was derived from a core, its composition should have been fractionated by this time. (Mesosiderite metal is not fractionated in siderophile elements.) Therefore, an alternative heat source has to be looked for. Here we report petrography of a mesosiderite which was largely molten by the reheating event, based on which we discuss the heating process.

NWA 2924 has not been studied in detail. But it is noteworthy that it suffered only minor shock effects (Meteoritical Bulletin). Two polished sections (one metal nodule and one matrix) were observed with a SEM and the mineral compositions were analyzed with an EDS. The areal silicate fractions are plagioclase=0.380, pyroxene=0.534 and silica=0.086. This corresponds to the type A mesosiderite. Sub-classification of mesosiderites by degrees of reheating is rather confusing [3]. In our opinion, melt-rock mesosiderites should be classified as type 3. (Type 4 is eliminated.) They can be easily distinguished from type 2 by the absence of olivine coronas and by the presence of silica/plagioclase needles that penetrate into metal. By this definition, NWA 2924 is a type 3A mesosiderite.

Chromite in NWA 2924 shows three types of petrographic features. (1) Some chromites contain ubiquitous spherical silicate inclusions. (2) Some chromites contain similar spherical silicate inclusions which are restricted to the outer part of the chromite grains. (3) Clusters of smaller chromite grains which do not include much silicate inclusions are present. Such clusters are often observed in silicate inclusions inside metal nodules. The spherical silicate inclusions are considered to be produced as follows. Chromite and surrounding silicates were heated to above the solidus temperatures of silicates, and chromite was dissolved into the silicate melt. Shortly afterwards, it cooled rapidly and silicate melt was trapped in the growing chromite. In case (1), the heating was just enough for complete melting of chromite. In case (2), only the outer part of chromite was dissolved. In case (3), chromite was completely dissolved and the dissolved chromite component diffused away considerably, so that new chromite grains formed upon individual nucleation sites (that are located nearby), resulting in a cluster of small chromites. Such chromite features are different from those in shock-heated chondrites [4]. In shocked chondrites, chromite appears as fine (micron size) granular fragments because it is brittle.

This petrographic observation is important in 3 ways. First, it suggests that the heating was very brief. Second, it seems that chromite in metal nodules was molten more extensively, suggesting different environment such as higher temperatures and/or different melt compositions and volumes than the matrix. Third, shock heating is an unlikely mechanism for reheating mesosiderites, although it may be preferred solely based on the briefness of the heating.

Since radiogenic heat, accreting hot metal and shock heating are all ruled out as a heat source for mesosiderite reheating, we suggest that induction heating due to changing solar-wind magnetic field

(joule heating by eddy current) is a plausible mechanism for mesosiderite reheating. We certainly need more observations of chromite in melt-rock mesosiderites and other shocked meteorites.

[1] M.Koike et al., G.R.L. 2017, in press. [2] M.K. Haba et al., 79th Metsoc, 2016, #6139. [3] R.Hewins, J.G.R.1984, 89, C289-C297. [4] X.Xie et al., Eur. J. Mineral. 2001, 13, 1177 - 1190.

キーワード：メソシデライト、再加熱、誘導

Keywords: mesosiderite, reheating, induction

変形微細組織から推察される火星隕石ナクライトの形成環境に関する考察

The consideration regarding formation environment of the nakhlite meteorites inferred from deformation microstructures

*高野 安見子¹、片山 郁夫¹、臼井 寛裕²、伊藤 元雄³、道林 克禎⁴

*Amiko Takano¹, Ikuo Katayama¹, Tomohiro Usui², Motoo Ito³, Katsuyoshi Michibayashi⁴

1. 広島大学大学院理学研究科地球惑星システム学専攻、2. 東京工業大学地球生命研究所、3. 海洋研究開発機構 高知コア研究所、4. 静岡大学学術院理学領域

1. Hiroshima University, 2. Earth-Life Science Institute, Tokyo Institute of Technology, 3. Kochi Institute for Core Sample Research JAMSTEC, 4. Institute of Geosciences, Shizuoka University

火星は太陽系内惑星の中で最も地球に似た特徴を持つ惑星として、近年多くの探査、研究が行われてきた。その結果、火星表面に関する知見は大幅に増加した。しかし、現状は火星表面の化学的分布とその場の地質学的な区分があまり一致していない可能性が示唆されている(西堀ほか, 2015)。このことから地表を覆う表土がその場の地質学的な履歴と関係がないということが火星地下浅部構造に関する研究の問題点として挙げられている。

本研究では、火星の地表面付近かつタルシス火山群由来と考えられている火星隕石ナクライト(Yamato 000593)を用い、火星表層付近の情報を直接的に得ることによって火星の地下浅部構造の形成環境についての考察を行なった。ナクライトはその鉱物組成を地球の岩石と比較することによって、溶岩流または浅い貫入岩の中で沈積し、形成されたと考えられているがその形成環境の詳細については未だに明らかにされていない(Treiman et al., 1987)。そのため隕石中の全岩での結晶方位を測定することにより、結晶沈積時の形成場の推察を行なった。その結果、Yamato 000593の主要鉱物である単斜輝石の方位について、3軸方向での集中が見られた。このことは、ナクライトの形成場は結晶の沈積時に結晶にせん断応力が作用する溶岩流のような応力場であったことを示唆する。

一方で、この岩石が火星から放出される際のインパクトの影響についても考察を行なった。輝石はインパクトによる変形時の情報を変形双晶などの形で記録している。そこで多くの単斜輝石中に形成されていた変形双晶の形成面を測定することによって、インパクトの影響について推察した。その結果、ほとんどの変形双晶が(100)面で形成されていた。(100)面での変形双晶は中程度の温度かつ高い歪み速度の条件で単斜輝石中に変形を誘発することでよく知られている(Leroux et al., 2004)。この結果を実験的に求められている単斜輝石のショックの影響と比較すると、Yamato 000593は強いインパクトの影響は受けていないということが考えられる。このことはカンラン石の破壊の程度などを用いて、火星から放出される際のYamato 000593に作用したインパクトの影響を調べている先行研究(Fritz et al., 2005)の結果とも一致している。

キーワード：ナクライト、結晶選択配向、形成環境、インパクトの影響

Keywords: nakhlite, crystal preferred orientation, formation environment, impact effect

Hydrogen Reservoirs in Mars as Revealed by SNC Meteorites

*臼井 寛裕¹

*Tomohiro Usui¹

1. 東京工業大学地球生命研究所

1. Earth-Life Science Institute, Tokyo Institute of Technology

The isotopic signatures of three hydrogen reservoirs are now identified based on analyses of Martian meteorites, telescopic observations, and Curiosity measurements: primordial water, surface water, and subsurface water (Usui, in press). The primordial water is retained in the mantle and has a D/H ratio similar to those seen in Martian building blocks (Usui et al. 2012). The surface water has been isotopically exchanged with the atmospheric water of which D/H ratio has increased through the planet's history to reach the present-day mean value of $\sim 5,000\%$ (Kurokawa et al. 2014). The subsurface water reservoir has intermediate δD values ($\sim 1,000$ - $2,000\%$), which are distinct from the low- δD primordial and the high- δD surface water reservoirs. We proposed that the intermediate- δD reservoir represents either hydrated crust and/or ground ice interbedded within sediments (Usui et al. 2015). The hydrated crustal materials and/or ground ice could have acquired its intermediate- δD composition from the ancient surface water reservoir (Usui et al. 2017).

References:

- Kurokawa, H. et al. (2014). Evolution of water reservoirs on Mars: Constraints from hydrogen isotopes in martian meteorites. *Earth Planet. Sci. Lett.* **394**, 179-185.
- Usui et al. (2012) Origin of water and mantle-crust interactions on Mars inferred from hydrogen isotopes and volatile element abundances of olivine-hosted melt inclusions of primitive shergottites. *Earth Planet. Sci. Lett.* **357-358**, 119-129.
- Usui et al. (2015) Meteoritic evidence for a previously unrecognized hydrogen reservoir on Mars. *Earth Planet. Sci. Lett.* **410**, 140-151.
- Usui et al. (2017) Hydrogen isotopic constraints on the evolution of surface and subsurface water on Mars. *The 48th Lunar Planetary Science Conference*, Abstract #1278.
- Usui et al. (in press) Hydrogen reservoirs in Mars as revealed by SNC meteorites. *Volatiles In The Martian Crust* (eds. Filiberoto J. and Schwenger S. P.), Elsevier B.V.

キーワード：水素同位体、火星隕石

Keywords: hydrogen isotope, Martian meteorites

Variations in Shock Deformation of Feldspars in Three Achondrites: NWA 2727 Lunar breccia, NWA 856 Shergottite and NWA 3117 Howardite.

*李在庸¹、Fagan Timothy²

*Jaeyong Lee¹, Timothy Fagan²

1. 東京大学大学院新領域創成科学研究科自然環境学専攻、2. 早稲田大学教育学部地球科学専修

1. Department of Environmental Studies, Graduate School of Frontier Sciences, The University of Tokyo, 2. Department of Earth Sciences, School of Education, Waseda University

In this study, I investigated shock history and geochemistry of three achondrite meteorites: NWA 3117, a howardite breccia from asteroid 4 Vesta; NWA 2727, a breccia from the Moon; and NWA 856, a shergottite from Mars. Shock histories of the three meteorites were evaluated from deformation of plagioclase feldspars. Geochemical study focused on electron microprobe (EPMA) analyses of pyroxene grains and use of Mn/Fe ratios to verify classification of these samples. Feldspar grains were classified based on observations in cross-polarized light as undulatory, mosaic, mosaic-recrystallized or maskelynite. This sequence represents increasing deformation of original feldspar crystals. Undulatory crystals have wavy extinction, mosaic crystals have patchy extinction, and mosaic-recrystallized grains appear as if they were originally coarse-grained and have recrystallized to mosaics of small equant crystals. Maskelynite grains are isotropic, indicating transformation to glass. Based on feldspar deformation, the degrees of impact processing are NWA 856 > NWA 3117 > NWA 2727. All of the feldspar observed in NWA 856 is maskelynite; mosaic and mosaic-recrystallized feldspars are common in NWA 3117; and the feldspar in NWA 2727 tends to have undulatory extinction.

The high deformation of NWA 856 is expected because this sample is from Mars, which is a large parent body and requires a powerful impact to accelerate a rock to escape velocity. In contrast, the parent body of NWA 3117 (Vesta) is smaller than that of NWA 2727 (the Moon), yet NWA 3117 appears more highly deformed than NWA 2727. One possible explanation is that NWA 2727 is from a relatively young part of the Moon, which has not been exposed to impacts as long as the surface of Vesta. My EPMA analyses of pyroxenes show that Mn/Fe ratios are highest in NWA 3117, lower in NWA 856, and lowest in NWA 2727, and are consistent with classification of these meteorites as a howardite (parent body Vesta), shergottite (Mars), and lunar meteorite (Moon), respectively. The higher volatility of Mn vs. Fe suggests that the observed variations in Mn/Fe could result from parent body formation at temperatures that were highest for the Moon, lower for Mars, and lowest for Vesta. However, variations in oxygen fugacity and other parameters may also have affected Mn/Fe.

キーワード：ハワードイト隕石、シャーゴットイト隕石、角礫月隕石、衝撃変形、長石、EPMA分析
Keywords: Howardite, Shergottite, Lunar breccia, Shock deformation, Feldspar, EPMA Analysis

木星型惑星の重水素核融合爆発による小惑星帯の形成説の検証

Validation on the scenario of the formation of asteroid belt by deuterium fusion explosion of Jupiter-like planet

*唐澤 信司¹

*Shinji Karasawa¹

1. 宮城工業高等専門学校 名誉教授

1. Miyagi National College of Tecnology Professor emeritus

太陽の質量の1.3%を超える天体は一時的に重水素が核融合することができます[1]。この天体の中心の重力ポテンシャルを密度一定として計算すると対応する重水素の温度は約百万度(10^6 K)になります。重力により天体を取り込む量より核融合で加熱され放出される量の方が多く、その放出が一度に起ればその天体は爆発します。そこで、太陽系の氷結線(4.04×10^8 km. 文献[2])の少し外側のケレスの位置(小惑星帯の中央: 4.14×10^8 km)にあった惑星(X)が太陽の質量の1.3%を持つまで成長して核爆発したとする説を検証しました。

太陽から惑星までの距離は次のようになります。海王星：45.04、天王星：28.75、土星：14.29、木星：7.78、惑星(X)：4.14、火星：2.27、地球：1.50 [10^8 km単位]。惑星の引力が太陽に向かって減少し、太陽の引力と等しくなる距離として引力圏を求めると次のようになります。海王星：0.32、天王星：0.19、土星：0.24、木星：0.24、惑星(X)：0.81、火星：0.013、地球：0.026 [10^8 km単位]。ここで、惑星(X)は質量が木星の13倍の木星型としました。惑星(X)が大きくなった理由は惑星(X)が氷結線のすぐ外側の位置したこと、宇宙塵の100倍もある星雲ガスが重力崩壊したことによります。

46億年前に太陽で核融合が始まったことも惑星(X)の成長に拍車をかけました。そして、惑星(X)において重水素の核融合が始まり、その核融合は爆発だけで終わったとします。鉄隕石は万有引力では形成も破壊もできません。太陽を公転する天体の軌道は質量に依存しません。核融合で固体のコアが爆発すると破片の大部分は宇宙に飛散します。残りの同じ公転軌道を公転し続ける惑星(X)の破片も弾性衝突で拡散しますが重心の運動は変わりません。この惑星(X)の重水素核融合による爆発が38億年前に起こったとすると地球のマントルの成分が示す隕石重爆撃も説明できます。

詳しくはWebsite； “https://youtu.be/medU_Rq6StI” , “<https://youtu.be/Kz8TTGICHXl>” をご覧ください。

[参考文献]

[1] Chabrier, G., Baraffe, I., Low-mass stars and substellar objects, *Ann. Rev. Astron. Astrophys.* 38 (2000) 337-377.

[2] Hayashi, C., *Prog. Theor. Phys. Suppt.*, Vol. 70, pp. 35-53.

キーワード：小惑星帯、隕石、重水素核融合、褐色矮星、木星、ケレス

Keywords: asteroid belt, meteorite, deuterium fusion, brown dwarf, Jupiter, Ceres

Effects of protoplanetary multiplicity and migration on late-stage accretion of solids onto gas giants

*Sho Shibata¹, Masahiro Ikoma¹, Yuhiko Aoyama¹

1. Graduate School of Science, The University of Tokyo

In recent years, many extrasolar gas giants have been discovered, and detailed observation reveals common characteristics of those gas giants. Their envelopes are thought to have come from protoplanetary disks, whose composition must be almost the same as that of central stars, namely, composed mainly of hydrogen and helium. Several studies of the bulk composition of gas giants, however, indicate that the envelopes of many gas giants, including Jupiter and Saturn, are much richer in heavy elements than the central stars. To explain the origin of the heavy elements, previous studies performed N-body simulations of planetesimals around growing gas giants and estimated the amount of heavy elements captured by gas giants. The estimated total masses are about a few Earth masses, which are too small to explain the observation. In this study, for the effects that enhance solid accretion, we take the multiplicity and migration of protoplanets into account. We demonstrate that the existence of another protoplanet can help supplying planetesimals to the protoplanet by scattering and also protoplanetary migration enhances the capture of planetesimals by sweeping. As a result, since planetesimals in broader area are captured by the planet, the envelopes end up being richer in heavy elements than previously thought.

Keywords: Heavy Elements, Planet Formation, Extrasolar Planet

惑星集積メカニズムの謎と起源,月の起源,小惑星帯,コアリッチ水星,全ての起源と謎をマルチインパクト仮説で一度きりの進化を利用して, アブダクションを適用し統一的に証明された.

それは過去の起源を解明する画期的な方法である.

Mystery of Planetary Integration Mechanism, and Origin of Moon, Asteroid Belt, Core Rich Mercury,

Mystery and all Origins were unified proved by Application of Abduction at One-case Evolution with “Multi-Impact Hypothesis” to Past.

*種子 彰¹

*Akira Taneko¹

1. SEED SCIENCE Lab.

1. SEED SCIENCE Lab.

ティティウス・ボーデの法則は証明できていない経験則です。しかし、此の法則は惑星相互の衝突合体の必要条件を示唆しています。円軌道の粒子と楕円軌道の粒子が遠点位置で速度差が殆ど無く接線衝突する場合は、合体して熱エネルギーだけ速度は低下する。

ティティウス・ボーデの法則では軌道半径は $R_n = R_{ex} (0.4 + 0.4 \times 2^{(n-1)})$ と表わされる。但し $R_{ex} = 149,597,870.700 \text{ km}$: 一天文単位 $n=1$ 水星 $n=2$ 金星 $n=3$ 地球 $n=4$ 火星 $n=5$ セレス $n=6$ 木星 $n=7$ 土星 $n=8$ 天王星 この辺で怪しくなってくる

ジャイアントインパクト仮説のシミュレーションではマントル成分だけの月形成が計算されたが、月の軌道エネルギーは現実の1/20しか得られなかった。アブダクションの考え方では現状を説明できると信頼性は増すが、説明できないと怪しさが増す。マルチインパクト仮説では、プレートテクトニクスと深海洋底と環太平洋弧状列島の起源地軸傾斜とバンアレン帯偏芯の起源とプレートテクトニクスの新駆動力の全てを統一的に説明出来たので、一度だけの地球の進化・歴史により検証しえたと云える。

更に、マルチインパクト仮説では小惑星帯の起源や分化した隕石の起源、木星大赤斑や冥王星の起源、海王星の地軸の傾きや水星のコア・マントル比の大きい起源も説明できます。この様に地球だけでなく太陽系の起源と進化も統一的に説明できます。

太陽系物理での起源の解明は、再現実験は不可能であり、帰納法や演繹法でも解明は困難である。

しかし、物理的に意義ある仮説を用いれば、太陽系の起源を初期条件も一致した一回だけの進化を利用して、複数の現状で完全に系統的にアブダクションにより説明できて検証できるので、より真実に近いと云えます。

根拠の無い偶然に頼る仮説のシミュレーションでは成果は少なく、且つ矛盾も多く得られる。具体的にはジャイアントインパクト仮説では、月の表面と裏面の密度の違いや隕石重爆撃期の起源も説明できない。

全ての起源はアブダクションで解明できる。他の証明は困難で有る

マルチインパクト仮説では更に、小惑星帯の起源やセラ位置の惑星の空白、水星のコア・マントル比が他の地球型惑星の二倍、木星の大赤斑の起源、冥王星の起源、ダイヤモンドの起源とキンバーライトパイプの起源、分化した地球隕石の謎、プレート移動方向急変の謎などを全て統一的に説明が可能である。

キーワード：惑星集積メカニズム、小惑星帯の起源、月の起源、木星大赤斑の起源、分化した小惑星、コア
リッチな水星

Keywords: Planetary accumulation mechanism, Origin of the asteroid belt, Origin of the Moon, Origin of
Large Red Spot, Differentiated asteroids, core rich Mercury

